Hany A. Elazab*, Sherif Moussa, Kendra W. Brinkley, B. Frank Gupton and M. Samy El-Shall

The continuous synthesis of Pd supported on Fe_3O_4 nanoparticles: a highly effective and magnetic catalyst for CO oxidation

DOI 10.1515/gps-2016-0168
Received October 4, 2016; accepted January 4, 2017; previously published online March 30, 2017

Abstract: We report a facile approach used for the simultaneous reduction and synthesis of a well dispersed magnetically separable palladium nanoparticle supported on magnetite (Pd/Fe_3O_4 nanoparticles) via continuous flow synthesis under microwave irradiation conditions, using a Wave Craft's microwave flow reactor commercially known as ArrheniusOne, which can act as a unique process for the synthesis of highly active catalysts for carbon monoxide (CO) oxidation catalysis. The prepared catalysts are magnetic, which is an advantage in the separation process of the catalyst from the reaction medium. The separation process is achieved by applying a strong external magnetic field which makes the separation process easy, reliable, and environmentally friendly. Hydrazine hydrate was used as the reducing agent under continuous flow reaction conditions. The investigated catalysis data revealed that palladium supported on iron oxide catalyst synthesized by continuous flow microwave irradiation conditions showed remarkable high catalytic activity towards CO oxidation compared to the ones that were prepared by batch reaction conditions under the same experimental conditions. This could be attributed to the high degree of dispersion and concentration ratio of the Pd nanoparticles dispersed on the surface of magnetite (Fe_3O_4) with a small particle size of 5–8 nm due to the effective microwave-assisted reduction method under continuous flow conditions. These nanoparticles were further characterized by a variety of spectroscopic techniques including X-ray photoelectron spectroscopy (XPS), X-ray diffraction (XRD), and transmission electron microscopy (TEM).

Keywords: CO catalytic oxidation; continuous flow chemistry; hydrazine hydrate; magnetite (Fe_3O_4); microwave heating; Pd-nanoparticles; solid supported catalysis.

***Corresponding author: Hany A. Elazab,** Chemical Engineering Department, The British University in Egypt (BUE), El Sherouk City Postal No. 11837, P.O. Box 43, Cairo 11837, Egypt; and Chemical Engineering Department, Virginia Commonwealth University (VCU), Richmond, VA, USA, e-mail: elazabha@mymail.vcu.edu
Sherif Moussa: Chemistry Department, Virginia Commonwealth University (VCU), Richmond, VA 23284-2006, USA
Kendra W. Brinkley and B. Frank Gupton: School of Engineering, Chemical Engineering Department, Virginia Commonwealth University (VCU), Richmond, VA 23284-3068, USA
M. Samy El-Shall: School of Engineering, Chemical Engineering Department, Virginia Commonwealth University (VCU), Richmond, VA 23284-3068, USA; and Chemistry Department, Virginia Commonwealth University (VCU), Richmond, VA 23284-2006, USA

1 Introduction

Magnetic nanoparticles have been recognized as a class of nanostructured materials of current interest due to outstanding physical and chemical properties, especially when used in combination with other metal nanoparticles [1–4]. These kinds of nanostructured materials play an important role not only in the field of catalysis, but also in many aspects of research ranging from catalysis and biology, to material science, advanced technological and medical applications, and green chemistry [5–17].

The metal oxide nanocatalysts are of great importance in improving the thermal-catalytic decomposition performance [18–20]. The advanced and unique magnetic, electronic, and catalytic properties of the materials in the nanoscale attracted research centers to investigate this area of science deeply [21–26]. In the field of catalysis, separation of catalysts is a vital step, especially in medical and therapeutic applications and mainly in cross coupling reactions [17, 27–37].

The catalytic effect of magnetic nanoparticles was an important area of research due to its huge industrial applications [38–40]. It is well known that one of the important issues in catalysis is catalyst separation, as catalysts that cannot be recovered or recycled from the reaction mixture are generally not preferred in chemical industry, even if they are highly active catalysts.

Recently, there has been an increasing trend towards using these kinds of magnetically recoverable nanomaterials in order to develop green chemical synthetic processes.

By using magnetic nanoparticles as a support, it is easy to recover those catalysts by applying a strong external magnetic field to benefit from the paramagnetic character of those kinds of supports. The carbon materials have an increasing importance in catalytic processes when used as catalyst supports, but there is also an endless effort to develop other kinds of supports like metal oxides [21, 41–49].

Compared to conventional methods used in synthesis of metal nanoparticles, microwave-assisted synthesis represents a unique approach that could be used for the synthesis of a variety of nanomaterials including metals, semiconductors, bimetallic alloys, and metal oxides with controlled shape and size, without using high temperature or high pressure reaction conditions. In the case of using microwaves, the heating process is performed by the interaction of the permanent dipole moment of the polar molecule with the high frequency electromagnetic radiation.

Carbon monoxide (CO) is a potentially fatal gas that can cause severe side effects and much more serious symptoms and in some cases, death. With oxidation catalysis over nanoparticle catalysts, CO removal is highly effective [50].

Hence, tremendous trials for development of new catalysts for low temperature CO oxidation are an essential trend nowadays to decrease pollution from an environmental point of view [51–56]. Oxidation catalysis usually requires the use of transition metals such as gold, palladium, ruthenium, platinum, iridium, and rhodium [57, 58]. All oxidation catalysts work the same way to transform CO into carbon dioxide, thus reducing or eliminating the potential risk of CO inhalation [59–63]. Microwave heating has been successfully used to synthesize bimetallic nanoalloys and nanoporous magnetic iron oxide microspheres for CO oxidation [64–67].

Cobalt, iron and nickel are mainly used as Fischer-Tropsch catalysts, while their magnetic characterization provides valuable information about catalyst reduction, sizes of ferromagnetic nanoparticles, and chemisorption on ferromagnetic materials [68–77]. Synthesis of nanoparticles with variable sizes has been intensively tried, particularly for magnetic iron oxides with namely maghemite (α-Fe_2O_3) and magnetite (Fe_3O_4) [78–86]. Those nanoparticles were used efficiently as magnetic recoverable catalysts for various applications [42, 87–94].

Recently, microreactor technology has the capacity to transform current batch nanoproduction practices into continuous processes with rapid, uniform mixing and precise temperature control [89, 95–138]. Furthermore, nanoparticles with smaller mean particle size and narrow particle size distribution have been developed with continuous flow microreactors compared to bulk batch reactors [136]. Finally, if we compare some reported systems used in synthesis of magnetic supported Pd nanoparticles with our adopted approach using a continuous flow microreactor, it is obvious that there are many advantages, such as lower complete conversion of CO at 137°C, easy control, high temperature adaptability, high yield, lower reaction time, and simple operation [139–141]. However, this approach still has also some disadvantages like wide size distribution as a result of poor mixing, contamination due to contact with channel walls, and clogging [97, 142–153].

2 Materials and methods

All chemicals were purchased and used as received without further purifications. Palladium nitrate (10 wt.% in 10 wt.% HNO_3, 99.999%) and hydrazine hydrate (80%, hydrazine 51%) were obtained from Sigma Aldrich, St. Louis, USA. Deionized water (H_2O, ~18 MΩ) was used for all experiments. A JEOL JEM-1230 electron microscope by JEOL USA, Inc was operated at 120 kV was used to obtain transmission electron microscopy (TEM) images. The X-ray photoelectron spectroscopy (XPS) analysis was executed on a Thermo Fisher Scientific ESCALAB 250 (MA, USA) using a monochromatic Al KR X-ray. The X-ray diffraction (XRD) patterns were measured at room temperature using an X'Pert PRO PANanalytical X-ray diffraction (Boulder, CO, USA) unit, with CuKα. For the CO catalytic oxidation, tests were carried out in a continuous fixed-bed quartz-tube reactor Type F21100 Tube Furnace (Sigma Aldrich, St. Louis, USA) under ambient pressure.

2.1 Catalyst preparation

2.1.1 Synthesis of Pd-Fe_3O_4 under batch reaction conditions: $Fe(NO_3)_3 \cdot 9H_2O$ (90 mg, 0.223 mmol) was dissolved in deionized water (50 ml) and sonicated for 1 h. Palladium nitrate (10 wt.% in 10 wt.% HNO_3, 99.999%, 200 µl) was added to the iron nitrate solution. Then, the whole mixture was stirred for 3 h followed by the addition of the reducing agent hydrazine hydrate (1 ml) at room temperature and once the solution was heated by microwave for 90 s under batch reaction conditions, the color changed to a dark black color, indicating the completion of the chemical reduction. Then, the final product was washed using hot deionized water two to three times, ethanol two to three times times, and then left to dry in an oven at 80°C.

2.1.2 Synthesis of Pd-Fe_3O_4 under flow reaction conditions: Different catalysts were prepared but using an alternative method that is completely different from the one used under batch reaction conditions. In this approach, the catalysts were prepared under flow reaction conditions using a WaveCraft's microwave flow reactor called ArrheniusOne, as shown in Figure 1. This technique was used to prepare the Pd/Fe_3O_4 catalyst in large amounts compared to small amounts that were prepared under batch reaction conditions and

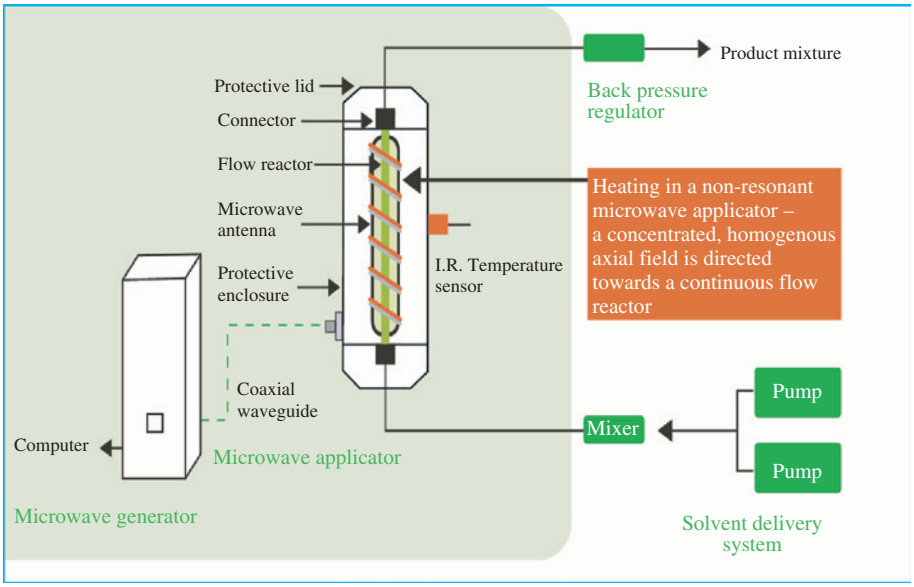

Figure 1: Wave Craft's ArrheniusOne microwave flow reactor.

also to produce a catalyst with the same specifications each time of preparation, in order to avoid problems of inconsistent specifications of different batches of catalysts that were prepared under batch reaction conditions. The ArrheniusOne unit is controlled and operated by the WaveCraft Control Application software program.

Figure 2 gives an overview of continuous flow microwave-assisted synthesis that is in many ways performed like conventional (convective heating) continuous flow synthesis. The main difference in this case is the speed of reaction, the simplicity in operating the system and the fact that there is no thermal wall effect due to the lack of physical contact between the reactor and the surroundings. Microwaves heat by a different mechanism than conventionally heated organic reactions.

Residence time is defined as the time when the reaction mixture is in the reaction zone exposed to microwaves. The residence time can be calculated using the following equation:

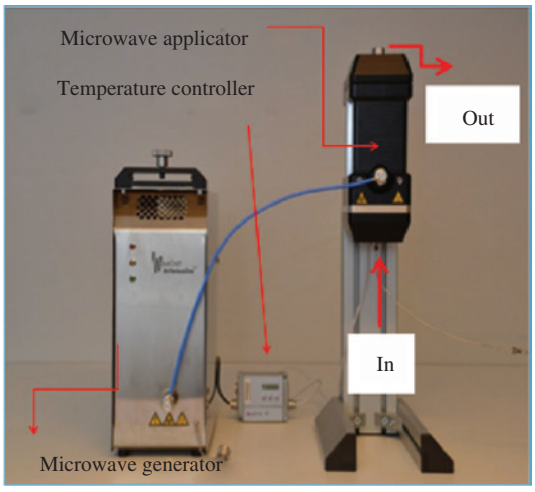

Figure 2: Continuous flow microwave-assisted synthesis (CF-MAS).

$$RT = \frac{L * (R^2 * \pi)}{F}$$

where RT is residence time in min, L is the length of the reactor in mm, R is the radius of the reactor in mm, F is the flow rate in micro l/min and π is 3.14.

The continuous flow microwave-assisted synthesis system consists of a microwave generator, an applicator to transfer the microwave energy to the reaction mixture, and a tubular borosilicate reactor in which the reaction mixture passes through the applicator (Figure 2) [152, 153].

In the axial field applicator the microwave field is generated in a coil surrounding the flow reactor as shown in Figure 3A and B, allowing the microwave field to be concentrated axially inside the coil. The coil is automatically tuned to maximize the heating in the reactor tube by changing the frequency. Figure 3C shows that reactors of different sizes can be used by changing the length and diameter of the coil in the applicator, allowing the optimization of reaction conditions such as residence time and flow capacity. The reactor consists of a straight tube, made of microwave-transparent borosilicate glass. As shown in Figure 3D after running the synthesis process, the reactor will have residual pressure due to the back pressure regulator. It is necessary to vent this pressure before disassembling the reactor.

Several different catalysts were prepared under different reaction conditions to investigate the optimum preparation method as in Tables 1–3.

In all catalysts prepared, a solution of $Fe(NO_3)_3 \cdot 9H_2O$(90 mg, 0.223 mmol) was dissolved in deionized water (50 ml) and sonicated for 1 h. Palladium nitrate (10 wt.% in 10 wt.% HNO_3, 99.999%, 200 µl) was added to the iron nitrate solution. Then, the whole mixture was stirred for 3 h. Similarly, another solution of hydrazine hydrate was mixed with deionized water to be used as a reducing solution for palladium nitrate-iron nitrate solution.

Different ratios of hydrazine hydrate-deionized water were prepared to investigate the effect of reducing agent concentration. Ratios used were (1 : 0.5, 0.5 : 1, and 1 : 1), and the prepared catalysts were checked for their catalytic activity as shown in Figure 4. The catalysts

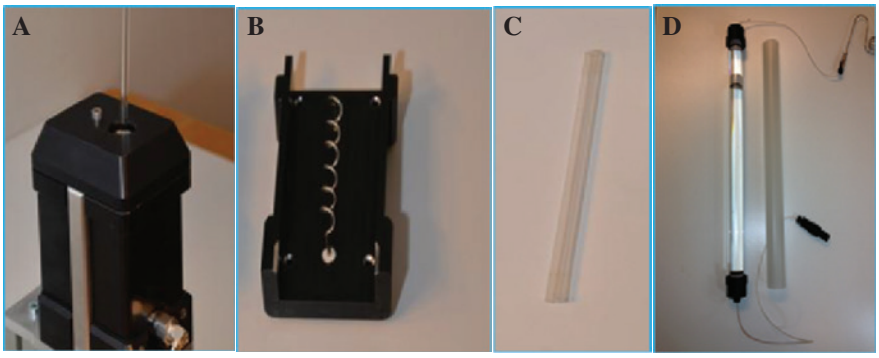

Figure 3: (A) Microwave applicator, (B) antenna casing, (C) 3 mm borosilicate glass reactor, (D) tube used for collecting the catalyst connected to a back pressure regulator.

Table 1: Selected Pd-Fe_3O_4 catalysts prepared at 80°C under flow reaction conditions.

Catalyst	1	2	3	4
Temperature (°C)	80	80	80	80
Flow rate of (Pd nitrate-Fe nitrate) (ml/min)	0.5	1	0.5	1
Flow rate of hydrazine hydrate (ml/min)	0.5	0.5	1	1
(Pd nitrate-Fe nitrate) : hydrazine hydrate	0.5 : 0.5	1 : 0.5	0.5 : 1	1 : 1
$T_{100\%}$ (°C)	254	200	190	168

Table 2: Selected Pd-Fe_3O_4 catalysts prepared at 150°C under flow reaction conditions.

Catalyst	6	7	8	9
Temperature (°C)	150	150	150	150
Flow rate of (Pd nitrate-Fe nitrate) (ml/min)	0.5	1	0.5	1
Flow rate of hydrazine hydrate (ml/min)	0.5	0.5	1	1
(Pd nitrate-Fe nitrate) : hydrazine hydrate	0.5 : 0.5	1 : 0.5	0.5 : 1	1 : 1
$T_{100\%}$ (°C)	210	177	160	137

Table 3: Comparison between selected Pd-Fe_3O_4 catalysts prepared under batch and flow reaction conditions.

Catalyst	4	5	9	10
Temperature (°C)	80	120	150	100
Flow rate of (Pd nitrate-Fe nitrate) (ml/min)	1	1	1	Batch reaction conditions
Flow rate of hydrazine hydrate (ml/min)	1	1	1	
(Pd nitrate-Fe nitrate) : hydrazine hydrate	1 : 1	1 : 1	1 : 1	–
$T_{100\%}$ (°C)	168	150	137	128

were prepared by injecting both (hydrazine hydrate-deionized water) solution and (palladium nitrate-iron nitrate) solution through using pumps to the T-Mixer where they were mixed together before being introduced to the microwave applicator where the reaction takes place inside a 3 mm reactor equipped from both sides with end sleeves made of Teflon material, for correct sealing of the fluidic system.

It is remarkable to notice that the color changed to a dark black color, indicating the completion of the chemical reduction. Then, the final product was washed using hot deionized water two to three times, ethanol two to three times, and then left to dry in an oven at 80°C.

2.1.3 General procedure for CO oxidation catalysis: Experiments for the CO catalytic oxidation were performed using a fixed bed-programmable flow tube furnace reactor (Thermolyne 2100) [64]. In a typical experiment, 20 mg of the test catalyst was dispersed in glasswool and placed inside a Pyrex glass tube. The sample and furnace temperatures were measured by a thermocouple placed in contact with the catalyst bed and in the middle of the tube furnace, respectively. Signals from thermocouples were processed using an SC-2345 data acquisition board. To plot temperatures and other measurement parameters, a data acquisition software using Labview was utilized. A gas mixture consisting of 4 wt.% CO and 20 wt.% O_2 in

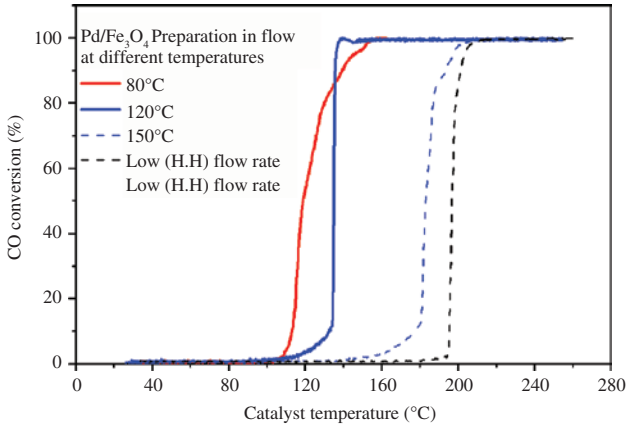

Figure 4: CO catalytic conversion of different catalysts of Pd/Fe_3O_4 Catalyst 4, Catalyst 5, Catalyst 9 at 80°C, 120°C, 150°C, respectively.

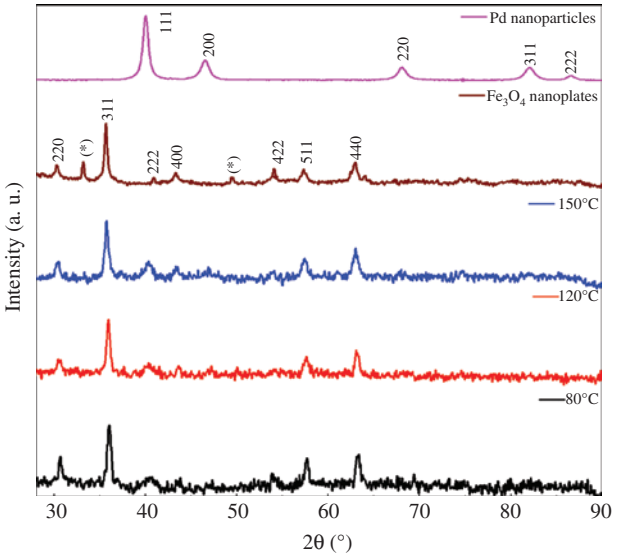

Figure 5: X-ray diffraction (XRD) pattern of palladium-Fe_3O_4 catalysts.

balance helium was passed over the sample at a flow rate of 100 cm^3/min, while the temperature was ramped.

The flow rate was controlled by a set of MKS digital mass flow meters. The conversion of CO to CO_2 was monitored using an online infrared gas analyzer (ACS, Automated Custom Systems Inc.) to detect the exit gas, which is then vented to an outlet. All the catalytic activities were measured after heat treatment of the catalyst at 110°C in the reactant gas mixture for 15 min in order to remove moisture and adsorbed impurities.

3 Results and discussion

Characterization of the Pd supported on Fe_3O_4 samples synthesized by the microwave irradiation method was examined in detail using XRD, XPS, and TEM analyses. The catalytic activities performance of different synthesized catalysts were evaluated towards CO oxidation catalysis. Comparing Catalyst 4, Catalyst 5, and Catalyst 9, which were prepared under the same flow reaction conditions but at different temperatures of 80°C, 120°C, and 150°C, respectively, Catalyst 9 was found to be the best catalyst for CO oxidation with 100% conversion to CO_2 at 137°C compared to 168°C and 150°C in the case of Catalyst 4 and Catalyst 5, respectively. This high catalytic activity of Catalyst 9 prepared under flow reaction conditions was very similar to that of Catalyst 10 that was prepared under batch reaction conditions.

The XRD patterns shown in Figure 5 revealed that the as-prepared catalysts are enriched with Fe_3O_4 and Pd(0). The diffraction peaks (2θ) of Pd-Fe_3O_4 at 40, 46.8, and 68.2 are ascribed to the (111), (200), and (220) planes of Pd NPs, respectively, which are similar to pure palladium with a characteristic sharp diffraction peak at $2\theta = 40°$, and a characteristic sharp diffraction peak of Fe_3O_4 is shown at $2\theta = 35°$ with reference code (ICCD-00-003-0863).

Figure 6 displays representative TEM images of the Pd-Fe_3O_4 catalysts. The TEM images show the presence of uniform well dispersed Pd nanoparticles on Fe_3O_4 as shown in Figure 7. However, the Pd nanoparticles supported on magnetite prepared under flow reaction conditions appear to be smaller than those prepared under batch reaction conditions as in Catalyst 6.

From those TEM images, it was found that for Catalyst 4, the particle size of Pd was 4–6 nm, while it was 11–13 nm for magnetite, as seen in Figure 6A. For Catalyst 5, the particle size of Pd was 5–7 nm, while it was 12–14 nm for magnetite, as seen in Figure 6B. For Catalyst 9, the particle size of Pd was 7–9 nm, while it was 16–18 nm for magnetite, as seen in Figure 6C. For Catalyst 10, the particle size of Pd was 12–14 nm, while it was 28–30 nm for magnetite as in Figure 6D.

The TEM-data also revealed that the Pd nanoparticles were smaller and well dispersed on the magnetite surface in the case of Catalyst 9 prepared by flow reaction conditions compared to the catalyst that was prepared under batch reaction conditions (Catalyst 10), which is a very important and decisive factor in catalysis. This is very consistent with the catalytic activity data obtained from experimental testing of those catalysts as previously mentioned in Table 3.

The XPS technique is more sensitive for the analysis of surface oxides than XRD. All the samples had a C1s binding energy around 284.5 eV derived from the carbon contamination in the analysis. Samples showed that the binding

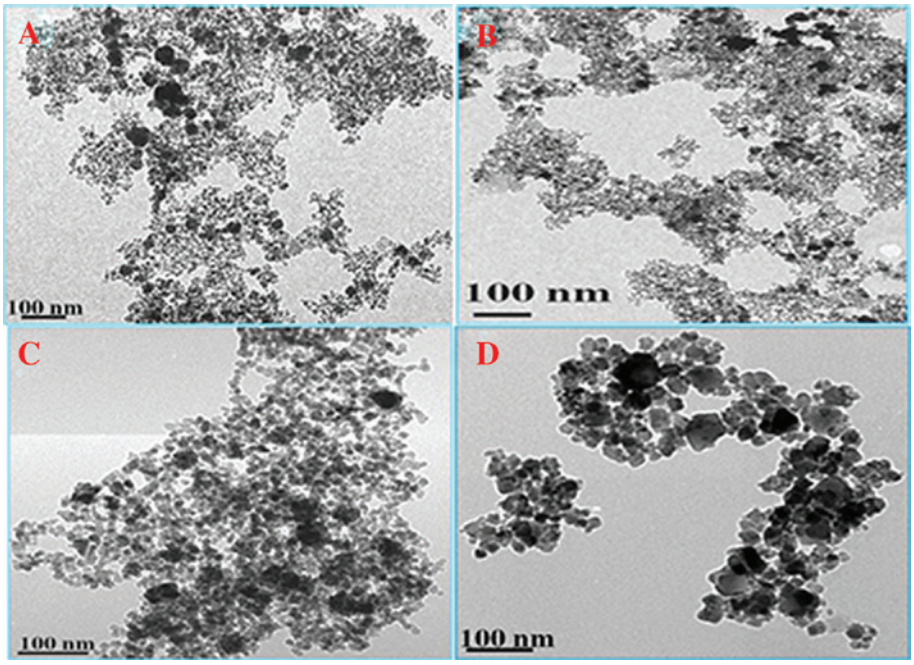

Figure 6: Transmission electron microscopy (TEM) images of different catalysts: (A) Catalyst 4, (B) Catalyst 5, (C) Catalyst 9, (D) Catalyst 10.

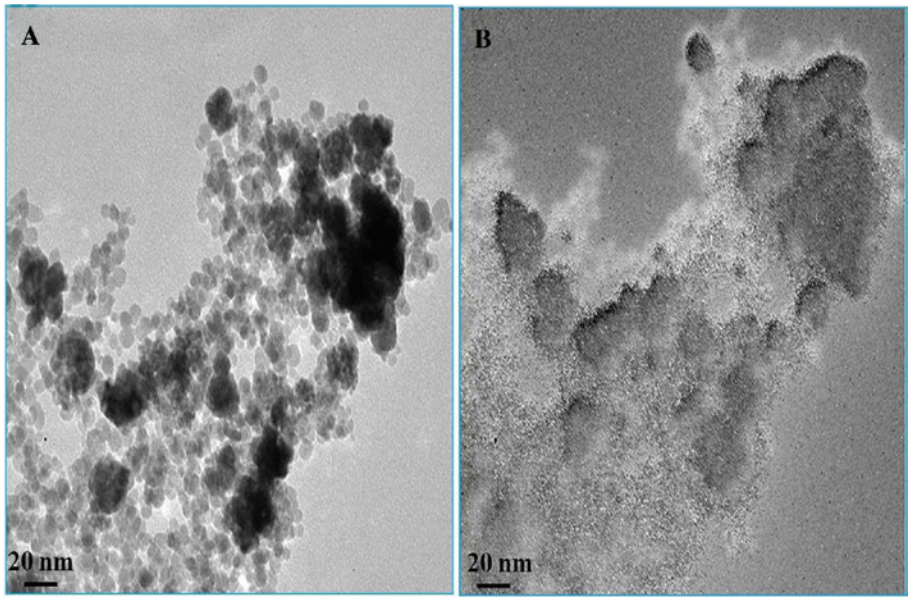

Figure 7: Transmission electron microscopy (TEM) images of iron mapping: (A) original image, (B) iron only "white sections".

energy (the energy difference between the initial and final states of the photoemission process) of the binding energy of Fe 2P 1/2 was 723.7 eV, indicating that Fe was present in the oxidation state of Fe_3O_4 and also the binding energy of Fe 2P 3/2 was 710.5 eV, indicating that the Fe was present as Fe_3O_4 as shown in Figure 8A.

The data reveal the presence of Fe(III) as indicated by the observed peaks at 724.2 eV and 710.5 eV corresponding to the binding energies of the 2p1/2 and 2p3/2 electrons, respectively. The broad Fe(III) 2p3/2 peak centered at 710.5 eV most likely contains contributions from the Fe(II) 2p3/2 which normally occurs at 708 eV.

In Figure 8B, it is so important to note that in the case of all catalysts, some of the Pd is in form of PdO or (Pd^{+2}) but some of the Pd is in the form of Pd^0. Also, the binding energy of Pd 3d5/2 was 335.14 eV, and Pd 3d3/2

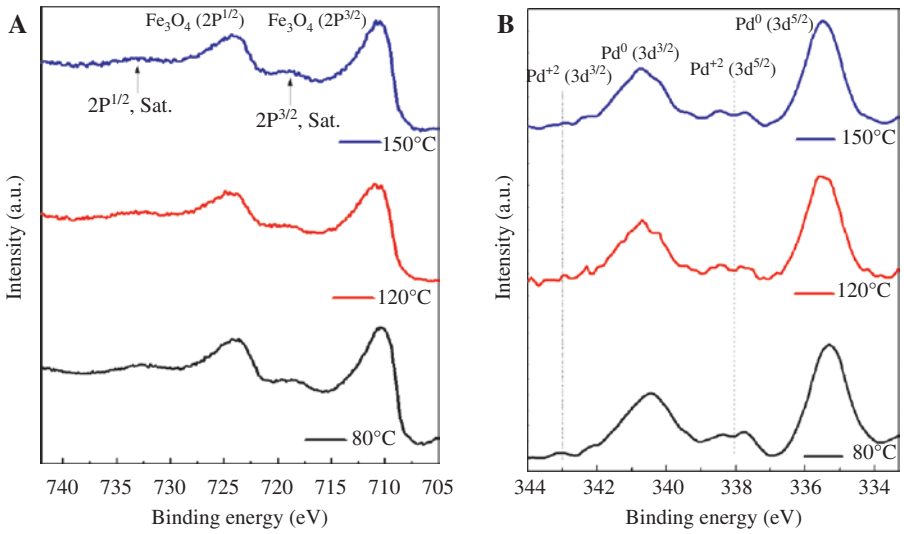

Figure 8: (A) X-ray photoelectron spectroscopy (XPS) binding energy (Fe 2p region) for the 50 wt.% Pd/Fe_3O_4 catalyst, (B) XPS binding energy (Pd 3d region) for the Pd/Fe_3O_4 catalysts prepared under flow reaction conditions.
Dashed lines show the locations of the 3d electron binding energies of Pd^{2+}.

Table 4: Pd(0) % to Pd(II) % for different selected catalysts of Pd-Fe_3O_4 prepared under batch and flow reaction conditions.

Catalyst	4	5	9	10
Pd(0) %	61	69	72	81.6
Pd(II) %	39	31	28	18.4
$T_{100\%}$ (°C)	168	150	137	128

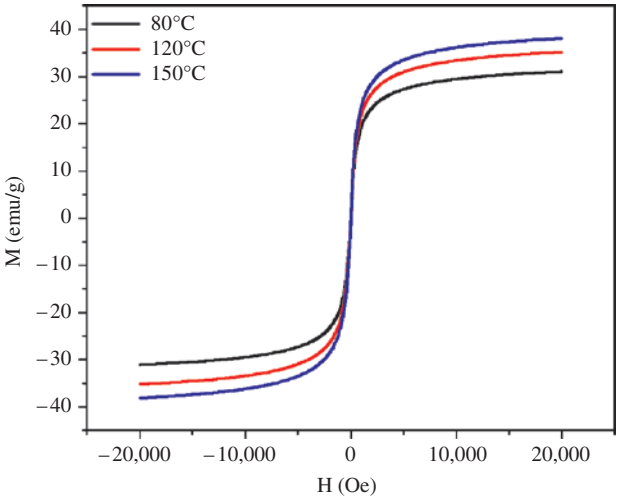

Figure 9: Magnetic hysteresis loops of Pd/Fe_3O_4 at room temperature after microwave irradiation (MWI).

was 340.57 eV corresponding to Pd^0. Similarly, the binding energy of Pd 3d3/2 was 343.2 eV and Pd 3d5/2 was 337.85 eV corresponding to Pd(II). Table 4 shows the percentage ratios of Pd(0) % to Pd(II) %.

As mentioned before in Figure 6, TEM images show that as the temperature increases, the particle size increases as well. So, it is obvious that a catalyst prepared at 80°C has a smaller particle size than a catalyst prepared at 120°C, which has also a smaller particle size than a catalyst prepared at 150°C. As a result, it can be observed that the saturation magnetization decreased as the size decreased. This agrees with the known fact that the magnetization of small particles decreases as the particle size decreases [154]. The magnetic properties of different catalysts were carried out by using vibrating sample magnetometer (VSM) analysis. Figure 9 presents the magnetic hysteresis loop of Pd-Fe_3O_4 and reveals the magnetic response of this catalyst to the varying magnetic field. It simply shows the hysteresis curves obtained for Pd-Fe_3O_4 different catalysts with an applied field sweeping from −40 kOe to 40 kOe. The hysteresis loop of the prepared samples reveal superparamagnetic behavior at room temperature with nearly zero coercivity and extremely low remnant magnetization values. The lack of remaining magnetization when the external magnetic field is removed is in agreement with a super paramagnetic behavior observed in magnetite nanosheets Fe_3O_4 decorated with Pd nanoparticles.

4 Conclusions

In conclusion, an application for a novel non-resonance microwave applicator was presented as the heating source in a continuous-flow synthesis system. This is a facile

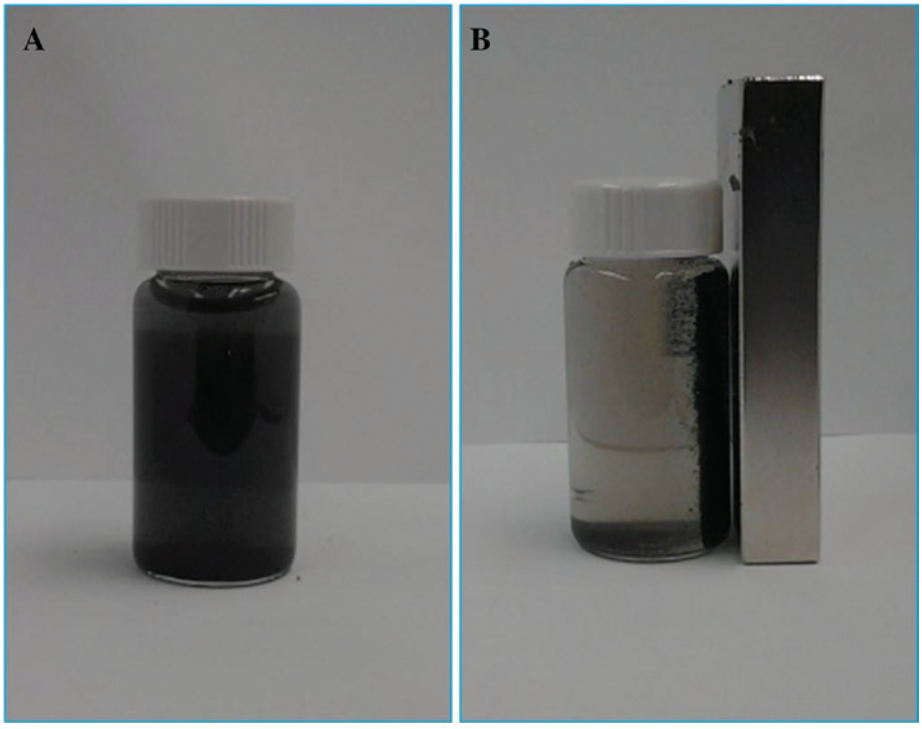

Figure 10: (A) Pd/Fe_3O_4 catalyst after preparation, (B) separating the catalyst by a strong magnet.

approach used for the synthesis of a well dispersed magnetically separable palladium supported on magnetite, which can act as a unique catalyst against CO oxidation catalysis due to the well dispersion of palladium nanoparticles throughout the magnetite surface.

The prepared catalysts were magnetic, which is an advantage in the separation process of catalyst from the reaction medium via applying a strong external magnetic field which makes the separation process easy, reliable and environmentally friendly as shown in Figure 10.

The typical synthesis was conducted under continuous flow reaction conditions by using hydrazine hydrate as a strong reducing agent for the reaction mixture under microwave irradiation synthesis. The palladium played a crucial role in the catalytic CO oxidation at low temperatures (100–137°C). Such a catalytic activity is supposed to be connected with the reaction between oxygen adsorbed on the reduced sites of the support and CO adsorbed on Pd at the metal oxide interface. The results would be useful for preparation of metal oxide catalysts under continuous flow reaction conditions with high performance at low temperatures.

It is important to mention that doping of Pd nanoparticles plays an important role to enhance the catalytic activity of Fe_3O_4 in CO catalytic oxidation by lowering the reaction temperature. However, the nature of the catalytic mechanism of such metal/metal oxide nanocomposites is still not scientifically clear. It is recommended that more experimental investigation is needed, particularly for evaluating the obtained theoretical calculations, in order to fully understand the catalytic reaction mechanism.

By applying the continuous flow method, the catalyst was prepared in larger amounts and in the same time without any differences in catalytic activity from batch to batch. In conclusion, an efficient magnetic catalyst has been successfully synthesized using a reliable, reproducible, fast and simple method using the microwave irradiation approach.

Acknowledgments: We would like to acknowledge Wave Craft's Company and Proteaf Technology Company for their support of this project. We also acknowledge Professor Dmitry Pestov and Professor Joseph Turner for their kind assistance in characterization. We gratefully acknowledge The British University in Egypt (Young Investigator Research Grant – YIRG 2016) for support of this work. We also express our deep gratitude to the National Science Foundation (CHE-0911146 and OISE-1002970) for support of this work.

Conflict of interest statement: The authors declare that there is no conflict of interest regarding the publication of this article.

[Conflict of interest statement added after ahead-of-print publication on 1 August 2017.]

References

[1] Nasrollahzadeh M, Atarod M, Sajadi SM. *J. Colloid Interface Sci.* 2017, 486, 153–162.
[2] Nasrollahzadeh M, Sajadi SM. *J. Colloid Interface Sci.* 2016, 464, 147–152.
[3] Nasrollahzadeh M, Bagherzadeh M, Karimi J. *J. Colloid Interface Sci.* 2016, 465, 271–278.
[4] Nasrollahzadeh M, Atarod M, Sajadi SM. *Appl. Surf. Sci.* 2016, 364, 636–644.
[5] Polshettiwar V, Varma RS. *Green Chem.* 2010, 12, 743–754.
[6] Yu XH, Hu YC, Zhou L, Cao FJ, Yang YX, Liang T, He JH. *Curr. Nanosci.* 2011, 7, 576–586.
[7] Xu ZW, Li H, Cao G, Cao Z, Zhang Q, Li K, Hou X, Li W, Cao W. *J. Mater. Chem.* 2010, 20, 8230–8232.
[8] Xia HQ, Cui B, Zhou J, Zhang L, Zhang J, Guo X, Guo H. *Appl. Surf. Sci.* 2011, 257, 9397–9402.
[9] Su QM, Li J, Zhong G, Du G, Xu B. *J. Phys. Chem. C* 2011, 115, 1838–1842.
[10] Rao PM, Zheng XL. *Nano Lett.* 2011, 11, 2390–2395.
[11] Coker VS, Bennett JA, Telling ND, Henkel T, Charnock JM, van der Laan G, Pattrick RA, Pearce CI, Cutting RS, Shannon IJ, Wood J, Arenholz E, Lyon IC, Lloyd JR. *ACS Nano* 2010, 4, 2577–2584.
[12] Atarod M, Nasrollahzadeh M, Mohammad Sajadi A. *J. Colloid Interface Sci.* 2016, 465, 249–258.
[13] Nasrollahzadeh M, Sajadib SM, Rostami-Vartoonia A, Khalaj M. *J. Mol. Catal. A: Chem.* 2015, 396, 31–39.
[14] Nasrollahzadeh M, Maham M, Rostami-Vartooni A, Bagherzadeh M, Sajadiet SM. *RSC Adv.* 2015, 5, 64769–64780.
[15] Nasrollahzadeh M, Azarian A, Maham M, Ehsani A. *J. Ind. Eng. Chem.* 2015, 21, 746–748.
[16] Atarod M, Nasrollahzadeh M, Sajadi SM. *RSC Adv.* 2015, 5, 91532–91543.
[17] Nasrollahzadeh M, Maham M, Ehsani A, Khalaj M. *RSC Adv.* 2014, 4, 19731–19736.
[18] Zhou ZX, Tian S, Zeng D, Tang G, Xie C. *J. Alloys Compd.* 2012, 513, 213–219.
[19] Xie XW, Shen WJ. *Nanoscale* 2009, 1, 50–60.
[20] Pan DK, Zhang H. *Chin. J. Inorg. Chem.* 2011, 27, 1341–1347.
[21] Alonso-Nunez G, de la Garza M, Rogel-Hernández E, Reynoso E, Licea-Claverie A, Felix-Navarro RM, Berhault G, Paraguay-Delgado F. *J. Nanopart. Res.* 2011, 13, 3643–3656.
[22] Xu MH, Xiao-Si Q, Wei Z, You-Wei D. *Chin. Phys. Lett.* 2009, 26, 103–116.
[23] Xiao CW, Ding H, Shen C, Yang T, Hui C, Gao H-J. *J. Phys. Chem C* 2009, 113, 13466–13469.
[24] Vaidya S, Ramanujachary KV, Lofland SE, Ganguli AK. *Cryst. Growth Des.* 2009, 9, 1666–1670.
[25] Salavati-Niasari M, Khansari A, Davar F. *Inorg. Chim. Acta* 2009, 362, 4937–4942.
[26] Senapati KK, Borgohain C, Phukan P. *J. Mol. Catal. A-Chem.* 2011, 339, 24–31.
[27] Liu W, Li B, Gao C, Xu Z. *Chem. Lett.* 2009, 38, 1110–1111.
[28] Zhu YH, Stubbs LP, Ho F, Liu R, Ship CP, Maguire JA. *Chemcatchem.* 2010, 2, 365–374.
[29] Zhang RZ, Liu J, Wang S, Sun W. *Chemcatchem.* 2010, 3, 146–149.
[30] Vargas C, Balu AM, Campelo JM, Gonzalez-Arellano C, Luque R, Romero AA. *Curr. Org. Synth.* 2012, 7, 568–586.
[31] Rosario-Amorin D, Gaboyard M, Clérac R, Nlate S, Heuzé K. *Dalton Trans.* 2001, 40, 44–46.
[32] Nasrollahzadeh M, Maham M, Ehsani A, Khalaj M. *ChemInform* 2014, 45, 13–17.
[33] Nasrollahzadeh M, Azarian A, Ehsani A, Zahraei A. *Tetrahedron Lett.* 2014, 55, 2813–2817.
[34] Nasrollahzadeh M, Azarian A, Ehsani A, Zahraei A. *ChemInform* 2014, 45, 746–748.
[35] Nasrollahzadeh M, Azarian A, Ehsani A, Babaei F. *Mater. Res. Bull.* 2014, 55, 168–175.
[36] Elazab HA, Siamaki AR, Moussa S, Gupton BF, El-Shall MS. *Appl. Catal. A* 2015, 491, 58–69.
[37] Elazab H, Moussa S, Gupton BF, El-Shall MS. *J. Nanopart. Res.* 2014, 16, 1–11.
[38] Andrade AL, Souza DM, Pereira MC, Fabris JD, Domingues RZ. *J. Nanosci. Nanotechnol.* 2009, 9, 3695–3699.
[39] Yan JM, Zhang X-B, Han S, Xu Q. *J. Power Sources* 2009, 194, 478–481.
[40] Mori K, Yamashita H. *Phys. Chem. Chem. Phys.* 2010, 12, 14420–14432.
[41] Rodriguez-Reinoso F. *Carbon* 1998, 36, 159–175.
[42] Berry FJ, Smith MR. *Hyperfine Interact.* 1991, 67, 549–557.
[43] Scheuermann GM, Rumi L, Steurer P, Bannwarth W, Mülhaupt R. *J. Am. Chem. Soc.* 2009, 131, 8262–8270.
[44] Guillen E, Rico R, López-Romero JM, Bedia J, Rosas JM, Rodríguez-Mirasol J, Cordero T. *Appl. Catal. A* 2009, 368, 113–120.
[45] Karousis N, Tsotsou G-E, Evangelista F, Rudolf P, Ragoussis N, Tagmatarchis N. *J. Phys. Chem. C* 2008, 112, 13463–13469.
[46] Li ZC, Zhou QF. *Rare Metal Mat. Eng.* 2007, 36, 1685–1688.
[47] Zhang Y, Chu W, Xie L, Sun W. *Chinese J. Chem.* 2010, 28, 879–883.
[48] Liu XS, Hu F, Zhu D-R, Jia D-N, Wang P-P, Ruan Z, Cheng C-H. *J. Alloys Compd.* 2011, 509, 2829–2832.
[49] Cao GX, Fu Y-W, Sun H-H, Xu Z-W, Li H-J, Tian S. *Chin. J. Inorg. Chem.* 2015, 27, 1431–1435.
[50] Yamada Y, Ueda A, Zhao Z, Maekawa T, Suzuki K, Takada T, Kobayashi T. *Catal. Today* 2001, 67, 379–387.
[51] Kudo S, Maki T, Yamada M, Mae K. *Chem. Eng. Sci.* 2010, 65, 214–219.
[52] Zou ZQ, Meng M, Zha YQ. *J. Alloys Compound.* 2009, 470, 96–106.
[53] Kandalam AK, Chatterjee B, Khanna SN, Rao BK, Jena P, Reddy BV. *Surf. Sci.* 2007, 601, 4873–4880.
[54] Dong J, Xu ZH, Kuznicki SM. *Adv. Funct. Mater.* 2009, 19, 1268–1275.
[55] Tsoncheva T, Manova E, Velinov N, Paneva D, Popova M, Kunev B, Tenchev K, Mitov I. *Catal. Commun.* 2001, 12, 105–109.
[56] Shen HY, Sheng-Dong P, Fang F, Jia S. In *New and Advanced Materials, Pts 1 and 2*, Zhou HY, Gu T, Yang D, Jiang Z, Zeng J, Eds., Trans Tech Publications: Giulin, China, 2011, pp. 495–498.
[57] Baruwati B, Polshettiwar V, Varma RS. *Tetrahedron Lett.* 2009, 50, 1215–1218.
[58] Sreedhar B, Kumar AS, Yada D. *Synlett* 2011, 8, 1081–1084.
[59] Ananikov VP, Orlov NV, Beletskaya IP, Timofeeva T. *J. Am. Chem. Soc.* 2007, 129, 7252.
[60] Moreno-Manas M, Pleixats R. *Accounts Chem. Res.* 2003, 36, 638–643.
[61] Tanikawa K, Egawa C. *Appl. Catal. A* 2011, 403, 12–17.
[62] Slavinskaya EM, Gulyaev RV, Stonkus O, Boronin AI. *Kinet. Catal.* 2011, 52, 282–295.

[63] Cargnello M, Wieder NL, Montini T, Fornasiero P. *J. Am. Chem. Soc.* 2010, 132, 1402–1409.
[64] Abdelsayed V, Aljarash A, El-Shall MS. *Chem. Mater.* 2009, 21, 2825–2834.
[65] Yang DP, Gao F, Cui D-X, Yang M. *Curr. Nanosci.* 2009, 5, 485–488.
[66] Yamauchi T, Tsukahara Y, Yamada K, Wada Y. *Chem. Mater.* 2011, 23, 75–84.
[67] Wu KL, Tsukahara Y, Yamada K, Wada Y. *J. Phys. Chem. C* 2011, 115, 16268–16274.
[68] Chernavskii PA, Dalmon J-A, Perov NS, Khodakov A. *OGST* 2009, 64, 25–48.
[69] Wang HZ, Kou X, Zhang L, Li J. *Mater. Res. Bull.* 2008, 43, 3529–3536.
[70] Zhang DE, Yang W, Wang MY, Zhang XB, Li SZ, Han GQ, Ying AL, Tong ZW. *J. Phys. Chem. Solids* 2011, 72, 1397–1399.
[71] Yang YZ, Liu X, Han Y, Ren W, Xu B. *J. Nanomater.* 2011, 2011, P1.
[72] Surowiec Z, Gac W, Wiertel M. *Acta Phys. Pol. A* 2010, 119, 18–20.
[73] Senthilkumar B, Selvan RK, Vinothbabu P, Erelshtein I, Gedanken A. *Mater. Chem. Phys*. 2011, 130, 285–292.
[74] Prakash I, Nallamuthu N, Muralidharan P, Venkateswarlu M, Misra M, Mohanty A, Satyanarayana NE. *J. Sol-Gel Sci. Technol.* 2011, 58, 24–32.
[75] Guo Y, Azmat MU, Liu X, Ren J, Wang Y, Lu G. *J. Mater. Sci.* 2011, 46, 4606–4613.
[76] Feng C, Zhang Y, Zhang Y, Wen Y, Zhao J. *Catal. Lett.* 2011, 141, 168–177.
[77] Chen L, Zhu Q, Hao Z, Zhang T, Xie Z. *Int. J. Hydrogen Energy* 2010, 35, 8494–8502.
[78] Zhang YX, Yu X-Y, Jia Y, Huang X. *Eur. J. Inorg. Chem.* 2011, 5096–5104.
[79] Zhang YQ, Wei XW, Yao ZJ. *Chin. J. Chem.* 2010, 28, 2274–2280.
[80] Qiu GH, Huang H, Genuino H, Suib SL. *J. Phys. Chem C* 2011, 115, 19626–19631.
[81] Qi G, Liu W, Bei ZN. *Chin. J. Chem.* 2011, 29, 131–134.
[82] Nasr-Esfahani M, Hoseini SJ, Mohammadi F. *Chin. J. Catal.* 2011, 32, 1484–1489.
[83] Nakhjavan B, Tahir MN, Panthöfer M, Gao H, Schladt TD, Gasi T, Ksenofontov V, Branscheid R, Weber S, Kolb U, Schreiber LM, Tremel W. *J. Mater. Chem*. 2011, 21, 6909–6915.
[84] Lu HY, Yang S-H, Deng J, Zhang Z-H. *Austr. J. Chem.* 2010, 63, 1290–1296.
[85] Liu B, Zhang W, Yang F, Feng H, Yang X. *J. Phys. Chem C* 2011, 115, 15875–15884.
[86] He LH, Yao L, Liu F, Huang W. *J. Nanosci. Nanotechnol*. 2010, 10, 6348–6355.
[87] He HK, Gao C. *J. Nanomater.* 2011, 2011, 397–404.
[88] Han Y, Wang Y, Li L, Wang Y, Jiao L, Yuan H, Liu S. *Electrochim. Acta* 2011, 56, 3175–3181.
[89] Frost CG, Mutton L. *Green Chem.* 2010, 12, 1687–1703.
[90] Firouzabadi H, Iranpoor N, Gholinejad M, Hoseini J. *Adv. Synth. Catal.* 2010, 353, 125–132.
[91] Fihri A, Bouhrara M, Nekoueishahraki B, Polshettiwar V. *Chem. Soc. Rev.* 2011, 40, 5181–5203.
[92] Falcon H, Tartaj P, Rebolledo AF, Campos-Martín JM, Fierro JLG, Al-Zahrani SM. In *Scientific Bases for the Preparation of Heterogeneous Catalysts: Proceedings of the 10th International Symposium*, Gaigneaux E, Devillers M, Hermans S, Jacobs PA, Martens J, Ruiz P, Eds., Louvain la Neuve, Belgium, 2010, pp. 347–350.
[93] Chen HM, Chu PK, He J, Hu T, Yang M. *J. Colloid Interface Sci.* 2011, 359, 68–74.
[94] Arundhathi R, Damodara D, Likhar PR, Kwon SH. *Adv. Synth. Catal.* 2011, 353, 1591–1600.
[95] Chang CH, Paul BK, Remcho VT, Atre S, Hutchison JE. *J. Nanopart. Res*. 2008, 10, 965–980.
[96] Knapkiewicz P. *J. Micromech. Microeng*. 2013, 23.
[97] Watts P, Wiles C. *J. Chem. Res.* 2012, 4, 181–193.
[98] Heinrich S, Edeling F, Liebner C, Hieronymus H, Lange T, Klemm E. *Chem. Eng. Sci.* 2012, 84, 540–543.
[99] Han SY, Paul BK, Chang CH. *J. Mater. Chem*. 2012, 22, 22906–22912.
[100] Gjuraj E, Kongoli R, Shore G. *Chem. Biochem. Eng. Q.* 2012, 26, 285–307.
[101] Fuse S. *J. Synth. Org. Chem. Jpn*. 2012, 70, 177–178.
[102] Chen YZ, Su Y, Jiao F, Chen G. *Rsc Adv.* 2012, 2, 5637–5644.
[103] Borovinskaya ES, Reschetilowski W. Russ. *J. Gen. Chem.* 2012, 82, 2108–2115.
[104] Aymonier C, Marre S, Loppinet-Serani A. *Actual. Chim.* 2012, 369, 17–23.
[105] Wiles C, Watts P. *Beilstein J. Org. Chem.* 2011, 7, 1360–1371.
[106] Schaber SD, Gerogiorgis DI, Ramachandran R, Evans JMB, Barton PI, Trout BL. *Ind. Eng. Chem. Res*. 2011, 50, 10083–10092.
[107] Pashkova A, Greiner L. *Chem. Ing. Tech*. 2011, 83, 1337–1342.
[108] Pagano N, Herath A, Cosford NDP. *Abstr. Pap. Am. Chem. Soc.* 2011, 242, 405–413.
[109] Oelgemoller M, Shvydkiv O. *Molecules* 2011, 16, 7522–7550.
[110] Munoz JD, Alcázar J, de la Hoz A, Díaz-Ortiz A. *Tetrahedron Lett.* 2011, 52, 6058–6060.
[111] Kockmann N, Roberge DM. *Chem. Eng. Process.* 2011, 50, 1017–1026.
[112] Glasnov TN, Kappe CO. *Chem. Eur. J.* 2011, 17, 11956–11968.
[113] Bothe D, Lojewski A, Warnecke HJ. *Chem. Eng. Sci.* 2011, 66, 6424–6440.
[114] Tu ST, Yu X, Luan W, Löwe H. *Chem. Eng. J.* 2010, 163, 165–179.
[115] Gross A, Schneider S, Abahmane L, Köhler JM. *Chem. Ing. Tech.* 2010, 82, 1789–1798.
[116] Fortunak J, Confalone PN, Grosso JA. *Curr. Opin. Drug Discov. Devel.* 2010, 13, 642–644.
[117] Dubnack K, Körsten S, Kreisel G, Frank T. *Chem. Ing. Tech.* 2010, 82, 1807–1812.
[118] Wiles C, Watts P. *Chim. Oggi.* 2009, 27, 34–36.
[119] Pont J. *Chim. Oggi.* 2009, 27, 3–3.
[120] Mak XY, Laurino P, Seeberger PH. *Chim. Oggi.* 2009, 27, 15–17.
[121] Chin P, Barney WS, Pindzola BA. *Curr. Opin. Drug Discov. Devel.* 2009, 12, 848–861.
[122] Wiles C, Watts P. *Eur. J. Org. Chem.* 2008, 10, 1655–1671.
[123] Singh BK, Kaval N, Tomar S, Van der Eycken E, Parmar VS. *Org. Process Res. Dev.* 2008, 12, 468–474.
[124] Wiles C, Watts P. *Expert Opin. Drug. Discov.* 2007, 2, 1487–1503.
[125] Watts P, Wiles C. *Chem. Commun.* 2007, 5, 443–467.
[126] LaPorte TL, Wang C. *Curr. Opin. Drug Discov Devel*. 2007, 10, 738–745.
[127] Kohler JM, Held M, Hübner U, Wagner J. *Chem. Eng. Technol.* 2007, 30, 347–354.
[128] Klemm E, Döring H, Geisselmann A, Schirrmeister S. *Chem. Eng. Technol.* 2007, 30, 1615–1621.
[129] Baxendale IR, Hayward JJ, Ley SV. *Comb. Chem. High Throughput Screening* 2007, 10, 802–836.

[130] Brivio M, Verboom W, Reinhoudt DN. *Lab Chip* 2006, 6, 329–344.
[131] Shchukin DG, Sukhorukov GB. *Adv. Mater.* 2004, 16, 671–682.
[132] Pennemann H, Watts P, Haswell SJ, Holger L. *Org. Process Res. Dev.* 2004, 8, 422–439.
[133] Holladay JD, Wang Y, Jones E. *Chem. Rev.* 2004, 104, 4767–4789.
[134] Hernandez EA, Delgado R, Castro ME. *Abstr. Pap. Am. Chem. Soc.* 2004, 227, U615–U615.
[135] Ehrfeld W, Hessel V, Lehr H. In *Microsystem Technology in Chemistry and Life Science*, Manz A, Becker H, Eds., Springer: Berlin, Heidelberg, Germany, 1998, pp. 233–252.
[136] Zhao CX, He L, Qiao SZ, *Chem. Eng. Sci.* 2011, 66, 1463–1479.
[137] Simmons M, Wiles C, Rocher V, Watts P. *J. Flow Chem.* 2013, 3, 7–10.
[138] Costantini F, Benetti EM, Tiggelaar RM, Gardeniers HJGE, Reinhoudt DN, Huskens J, Vancso J, Verboom W. *Chem. Eur. J.* 2013, 16, 12406–12411.
[139] Guo W, Jiao J, Tian K, Tang Y, Jia Y, Li R, Xu Z, Wang H. *RSC Adv.* 2015, 5, 102210–102218.
[140] Chen S, Si R, Taylor E, Chen J. *J. Phys. Chem. C* 2012, 116, 12969–12976.
[141] Jiang XC, Yu AB. *J. Mater. Process. Technol.* 2009, 209, 4558–4562.
[142] Tonhauser C, Natalello A, Löwe H, Frey H. *Macromolecules* 2012, 45, 9551–9570.
[143] Takebayashi Y, Sue K, Yoda S, Furuya T, Mae K. *Chem. Eng. J.* 2012, 180, 250–254.
[144] Sumino Y, Fukuyama T. *J. Synth. Org. Chem. Jpn.* 2012, 70, 896–907.
[145] Salic A, Tusek A, Zelic B. *J. Appl. Biomed.* 2012, 10, 137–153.
[146] Sadler S, Moeller AR, Jones GB. *Expert Opin. Drug Discov.* 2012, 7, 1107–1128.
[147] Rebrov EV. *J. Gen. Chem.* 2012, 82, 2060–2069.
[148] Peela NR, Lee IC, Vlachos DG. *Ind. Eng. Chem. Res.* 2012, 51, 16270–16277.
[149] Kirschning A, Kupracz L, Hartwig J. *Chem. Lett.* 2012, 41, 562–570.
[150] Hessel V, Gürsel IV, Wang Q, Lang J. *Chem. Ing. Tech.* 2012, 84, 660–684.
[151] Brinkley KW, Burkholder M, Siamaki AR, Gupton BF. *Green Process. Synth.* 2015, 4, 241–246.
[152] Ohrngren P, Fardost A, Russo F, Schanche J-S, Fagrell M, Larhed M. *Org. Process Res. Devel.* 2012, 16, 1053–1063.
[153] Gising J, Odell LR, Larhed M. *Org. Biomol. Chem.* 2012, 10, 2713–2729.
[154] Cao SW, Zhu YJ, Chang J. *New J. Chem.* 2008, 32, 1526–1530.

Bionotes

Hany A. Elazab

Hany A. Elazab is currently a lecturer at the Department of Chemical Engineering, British University in Egypt (BUE), Cairo, Egypt. He earned his PhD in chemical engineering from Virginia Commonwealth University (VCU) in Richmond, VA, USA. He is currently teaching courses in catalysis, thermodynamics, mass and energy balance. In 2016, he was awarded the Young Investigator Research Award (YIRG) from the BUE. His research interests include synthesis of nanomaterials, nanoalloys, nanoparticle catalysts, graphene, and graphene-supported catalysts.

Sherif Moussa

Sherif Moussa is an assistant professor in the Department of Chemistry, VCU. He earned his PhD from University of Missouri, Columbia, MO, USA and his MS from Imperial College, London, UK. He was also a Fulbright Visiting Scholar. His research interests include material chemistry, nanomaterials, and applied catalysis.

Kendra W. Brinkley

Kendra W. Brinkley received her PhD in May 2015. Kendra has been recognized with an Outstanding Teaching Assistant Award, and she is the recipient of a US Department of Education GAANN fellowship. As a doctoral student, she developed and taught a new course for freshmen CLSE majors and a summer chemistry class for the VCU Summer Transition Program, an NSF funded preparatory program for incoming underrepresented minority STEM majors.

B. Frank Gupton

B. Frank Gupton is a professor at VCU and holds joint appointments in the Department of Chemistry and the Department of Chemical and Life Science Engineering at VCU. He also serves as department chair of the Chemical and Life Science Engineering Department. Dr. Gupton's research group is currently focused on the development and evaluation of new heterogeneous catalysts that can be incorporated into continuous flow reactor systems for pharmaceutical applications.

M. Samy El-Shall

M. Samy El-Shall is the chairman of the Chemistry Department and a professor of chemistry and chemical engineering at VCU. He received his BS and MS degrees from Cairo University, and a PhD from Georgetown University. He did postdoctoral research in nucleation and clusters at UCLA. His research interests are in the general areas of molecular clusters, nucleation phenomena, nanostructured materials, graphene and nanocatalysis for energy and environmental applications. He has published over 230 refereed papers and review chapters, and he holds eight US patents on the synthesis of nanomaterials, nanoalloys, nanoparticle catalysts, graphene, and graphene-supported catalysts.